Results in Physics 6 (2016) 761–766

Contents lists available at ScienceDirect

Results in Physics

journal homepage: www.journals.elsevier.com/results-in-physics

Linear and nonlinear optical properties of Gd^{3+} doped zinc borotellurite glasses for all-optical switching applications

C. Eevon, M.K. Halimah *, A. Zakaria, C.A.C. Azurahanim, M.N. Azlan, M.F. Faznny

Physics Department, Faculty of Science, University Putra Malaysia, 43400 UPM Serdang, Selangor, Malaysia

ARTICLE INFO

Article history:
Received 4 August 2016
Received in revised form 14 September 2016
Accepted 6 October 2016
Available online 14 October 2016

Keywords:
Gadolinium
Rare earth
Borotellurite glass
Optical band gap
Refractive index
Nonlinear optical properties

ABSTRACT

In this work, linear and nonlinear optical parameters of zinc borotellurite glasses doped with Gd^{3+} have been studied for all-optical switching applications. A series of gadolinium zinc borotellurite glasses were synthesized by using conventional melt quenching technique. Optical absorption spectra were recorded by UV–vis spectroscopy. From the optical absorption spectra, the cut-off wavelength, optical band gap, Urbach energy and refractive index have been determined and are related to the structural changes in the glass systems. The nonlinear optical properties of Gd^{3+} doped glasses are investigated by using Z-scan technique. The values of nonlinear refractive index and absorption coefficient with closed and opened apertures of the Z-scan, respectively, were determined for proper utilization in nonlinear optical devices.

Introduction

Photonics materials with high third nonlinear optical properties have provided important information in the optical field for applications in all-optical switching device in optical telecommunication field. Host glasses such as tellurite glass contain unique properties such as low phonon energy, high refractive index and large third-order nonlinear susceptibility which with the presence of other modified matrices have been established to enhance the electrical conductivity, the relaxation strength and optical properties of the glass systems [1–3]. Optical glasses with large non-resonant nonlinear refractive indices are potential materials for all-optical switching devices and may also be used to enhance the performance of mode-lock solid-state laser [4].

Among all photonics materials, rare earth oxides glasses are found to have better third order nonlinear optical properties due to their fast response times, negligible linear loss and small two-photon absorption (TPA) in the wavelength range of interest [4]. The addition of rare earth oxide such as gadolinium oxide, Gd_2O_3 into glass network will cause enhancement in optical, physical and chemical properties of the glass such as greater hardness, greater thermal and elastic properties, higher chemical durability and show nonlinear optical properties [5]. In addition, Gd_2O_3 is a favorite material used for scintillating glasses to increase density and improve luminescent properties. Previously reported Gd_2O_3 containing glass by Binnemans et al. [6] shows that Gd^{3+} ions has strong emission around 310–312 nm which is very useful for producing narrow band UVB (ultraviolet broadband) light for medical application in treatment of skin diseases. Jimenez [7]. reported that addition of silver oxide to P_2O_5–BaO–Gd_2O_3 enhances the uv emission from Gd^{3+} ions which suggests potential UV type B luminescent materials for phototherapy lamps applications. However, there are very few studies on the linear and nonlinear optical properties of zinc borotellurite glasses doped with Gd_2O_3.

Nonlinear optical properties such as nonlinear refractive index, n_2 and nonlinear absorption coefficient, β can be measured by Z-scan technique, in which a sample is scanned near the focal region of a focused laser beam. When the sample is move along the propagation direction of the laser beam (Z-axis), it consequently experiences a phase and intensity modulation, which can be observed in the transmittance measured as a function of the sample position [8]. Bala et al. [4] shows that addition of Bi_2O_3 to ZnO–SiO_2 glasses caused the glass to have large nonlinear refractive index and comparatively small nonlinear absorption coefficient values which can be used for photonic application such as broadband optical amplifiers. The higher value of nonlinear refractive index obtained gives strong evidence of the contribution of

* Corresponding author.
E-mail address: hmk6360@gmail.com (M.K. Halimah).

http://dx.doi.org/10.1016/j.rinp.2016.10.010
2211-3797/

two-photon absorption of the glass and is due to highly polarizable oxide ions and high polarizability of cations. It was found by Chen et al. [16] that the third order nonlinear optical properties of the glass were investigated by using Z-scan technique and show that the high third order nonlinearity was due to high refractive index and small band gap.

Hence, the objective of this work is to study the effect of Gd_2O_3 on linear and nonlinear optical properties of zinc borotellurite glasses and to bring new information on optical and nonlinear optical properties to these glasses. The addition of Gd_2O_3 to the glass network is expected to increase the optical band gap and decrease the refractive index of the glass due to strong polarizing cation, Gd^{3+}. Besides, the addition of Gd_2O_3 to the vitreous network will enhance the nonlinear optical properties of the glass.

Experimental

The chemical formula is $\{[(TeO_2)_{70}(B_2O_3)_{30}]_{70}(ZnO)_{30}\}_{1-x}$-$(Gd_2O_3)_x$ where x = 1.0, 2.0, 3.0, 4.0 and 5.0 mol%. The raw materials in powder form used to synthesize glass sample are tellurium oxide, TeO_2 (Alfa Aesar, 99.99%), boron oxide, B_2O_3 (Alfa Aesar, 97.5%), zinc oxide, ZnO (Alfa Aesar, 99.99%) and gadolinium oxide, Gd_2O_3 (Alfa Aesar, 99.999%).

Glass of $\{[(TeO_2)_{70}(B_2O_3)_{30}]_{70}(ZnO)_{30}\}_{1-x}(Gd_2O_3)_x$ were synthesize using conventional melt-quenching techniques. Each of the raw materials used was weighed using electronic beam balance with an uncertainty of ±0.0001 g and was mixed using mortar pestle. After drying at 400 °C for an hour, these dried powders were melted in an alumina crucible at 900 °C for 3 h. In order to remove the residual stress, the glass lava was quickly pour into a stainless steel cylindrical shaped split mould that was preheated at 350 °C and was then annealed at 400 °C for an hour. Subsequently, the cooling furnace was switched off and the samples were allowed to cool down to ambient temperature overnight. All of the transparent glasses were cut into about 2 mm thickness sheets. The thickness of the glass was measured using vernier caliper with an accuracy of ±0.01 mm. Excessive glass samples were crushed for structural analysis.

The characteristic nature of gadolinium zinc borotellurite glasses were analyzed using X-ray diffraction which shows that the glass system yields broad diffusion hump that exhibits the amorphous nature of the materials. The structural change of Gd zinc borotellurite glasses was analyzed by Fourier transform infrared (FTIR) spectrometry at room temperature using Mattson 5000 FTIR spectrometer, in the wavenumber 4000–200 cm^{-1} and with resolution 2 cm^{-1}. The absorption spectra of the glasses were recorded in the range of 200–1000 nm using a Shimadzu-1650PC UV–vis spectrophotometer with the absolute accuracy in the wavelength of ±0.3 nm. The optical band gap, Urbach energy and refractive index were calculated from the experimental absorption spectra. The third-order nonlinearities including nonlinear refraction, n_2 and nonlinear absorption, β were determined on the basis of Z-scan measurement. Fig. 1 shows the schematic diagram of a single beam Z-scan experiment used in the present measurement. The experiments were performed using a 532 nm laser beam from a laser diode (Coherent Compass SDL-532-150T). The beam was focused to a small spot using a lens and the sample was moved along a Z-axis by a motorized translational stage. The transmitted light in the far field passes through the aperture and was recorded by a detector, D. The laser beam waist, w_o at the focus length was measured to be about 26.6 μm and the Rayleigh length was found to satisfy the basic criteria of the Z-scan experiment. All measurements were carried out at room temperature for both, closed and open aperture Z-scan experiment. The accuracy of this instrument is ±0.2%.

Results and discussion

Structural properties

The FTIR spectra of the present glass system are shown in Fig. 2. The spectra consist of strong absorption bands at 628–644 cm^{-1}, 899–906 cm^{-1}, 1039–1045 cm^{-1}, 1215–1222 cm^{-1} and 1344–1355 cm^{-1}. The observed IR bands and the band assignments are given in Table 1 and Table 2, respectively.

The band arounds 628 cm^{-1} is due to the stretching vibrations of Te–O in TeO_4 trigonal bipyramid (tbp) units. It is observed from Fig. 2 that the band shifts from 628 to 644 cm^{-1} as the Gd_2O_3 content is increased from 1.0–5.0 mol%. This observation suggests that the lower coordination TeO_3 units transformed into the higher coordination TeO_4 units with the addition of Gd_2O_3 content. The IR band of pure Gd_2O_3 is around 644 cm^{-1}. This suggests that the addition of Gd_2O_3 content caused axial symmetrical stretching vibration modes of TeO_4 tetrahedral units [9].

The IR band at around 899–907 cm^{-1}, 1039–1045 cm^{-1}, 1215–1222 cm^{-1} and 1344–1355 cm^{-1} are due to the B–O bond stretching vibration of BO_4 units and BO_3 units. The changes in wavenumber might be due structural changes attributed to the presence

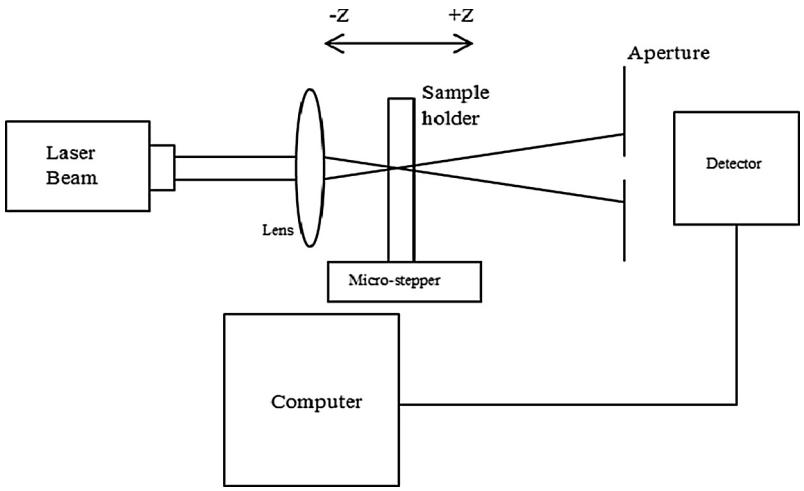

Fig. 1. Schematic diagram of a single beam Z-scan experiment.

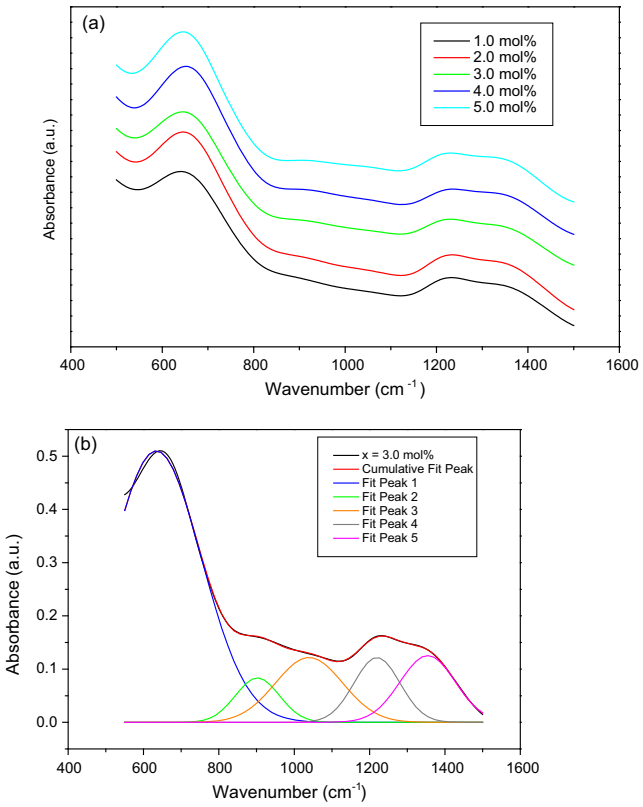

Fig. 2. (a) FTIR spectra for $\{[(TeO_2)_{70}(B_2O_3)_{30}]_{70}(ZnO)_{30}\}_{1-x}(Gd_2O_3)_x$ where x = 1.0, 2.0, 3.0, 4.0 and 5.0 mol% glasses and (b) deconvoluted FTIR spectrum for $\{[(TeO_2)_{70}(B_2O_3)_{30}]_{70}(ZnO)_{30}\}_{1-x}(Gd_2O_3)_x$ glass system with x = 3.0 mol%.

Gd^{3+} ions interacting with the oxygen of BO_4 units and stretching vibrations of triangular $(BO_3)^{3-}$ from various types of borate group [10].

The phonon energy of the glass host can be defined as the highest vibrational energy observed in the IR spectrum. Host materials having low phonon energy are useful for obtaining high-efficiency lasers and fiber amplifiers due to the reduction of non-radiative transitions and enhance the luminescence efficiency of dopant ions [11].

Linear optical properties

Fig. 3 shows the UV–vis optical absorption spectra of the presently studied glasses at room temperature. It is observed that the optical absorption edge is not sharply defined which indicates the amorphous nature of the samples. The cutoff wavelength, λ_c, shifted towards lower wavelength (blue shifted) as the content of Gd_2O_3 increases in the glass system. This is due to the formation of TeO_4 and BO_4 that modify the structure of the glass network [12–14]. Besides that, a small absorption band is observed in the range of between 300 and 400 nm. This might be due to

Table 2
Characteristic bands assignments TeO_2–B_2O_3–ZnO–Gd_2O_3 glass system.

Band frequency range (cm^{-1})	Assignments
628–644	Stretching vibrations [TeO_4]
899–907	Stretching vibrations of the non-bridging oxygens (NBO) of BO_4 groups
1039–1045	B–O stretching vibrations of BO_4 tetrahedra
1215–1222	Stretching vibrations of the B–O bonds of $(BO_3)^{3-}$ units involving mainly the linkage oxygen connecting different groups
1344–1355	Stretching vibrations of the B–O of trigonal $(BO_3)^{3-}$ units in metaborates, pyroborates and orthoborates

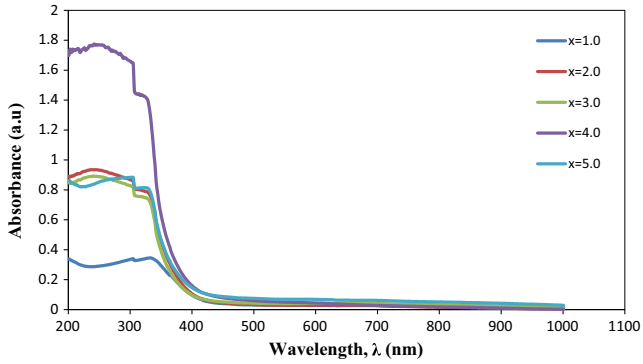

Fig. 3. Optical absorption spectra for TeO_2–B_2O_3–ZnO–Gd_2O_3 glasses.

$^6P_{7/2} \rightarrow {}^8S_{7/2}$ transitions suggesting a gadolinium-mediated energy transfer pathway [24]. The absorption band obtained in UV region can be used to predict the possible PL band.

The optical band gap, Urbach energy and refractive index for TeO_2–B_2O_3–ZnO–Gd_2O_3 glasses are obtained from UV–vis optical absorption spectra. The optical band gap of the glass system is closely associated to the energy gap between the valence and conduction band. The factor that affects the conduction band is the glass forming anions while the cations play an indirect and significant role [15]. An expression for the absorption coefficient, $\alpha(\omega)$, as a function of photon energy, $\hbar\omega$ for direct and indirect optical transitions given by Mott and Davis is shown in the following relation [12]:

$$\alpha(\omega) = \frac{A(\hbar\omega - E_g^{opt})^n}{\hbar\omega} \quad (1)$$

where A is a constant related to the extent of the band tailing, E_g^{opt} is optical band gap energy, $\hbar\omega$ is the incident photon energy, n is an index that characterizes the optical absorption process and is equal to ½, 2, 3/2 or 3 for direct allowed, indirect allowed, direct forbidden and indirect forbidden transitions respectively. The equation with n = 2 is used to denote the experimental results for amorphous materials and in this case, it applies to indirect transitions in materials [12,16].

Table 1
Deconvolution parameters of the FTIR spectra of the glasses under investigation. The band frequencies of TeO_2–B_2O_3–ZnO–Gd_2O_3 glass system.

x (mol%)	Band Frequencies				
	1	2	3	4	5
1.0	628.9	899.2	1039.8	1219.3	1347.5
2.0	635.3	900.2	1040.2	1220.8	1353.8
3.0	634.1	902.4	1039.5	1219.8	1354.4
4.0	643.2	906.0	1039.6	1221.7	1354.6
5.0	637.2	902.6	1044.5	1215.0	1344.7

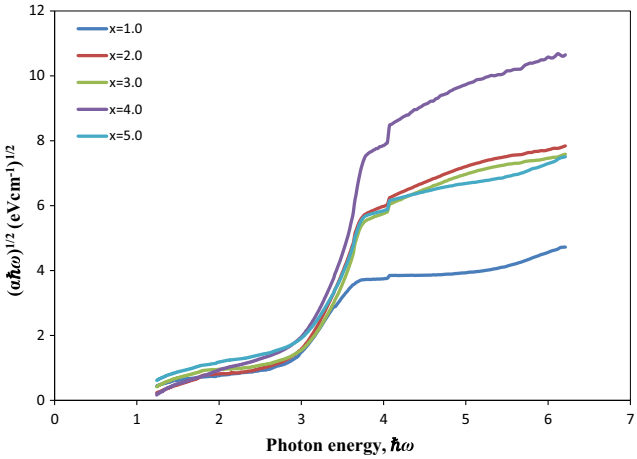

Fig. 4. Dependence of $(\alpha\hbar\omega)^{1/2}$ against ħω for TeO_2–B_2O_3–ZnO–Gd_2O_3 glasses.

Fig. 4 shows plot of $(\alpha(\omega)\hbar\omega)^{1/2}$ against ħω in eV units of glass samples. The optical band gap can be attained by extrapolating the linear curve to zero absorption. The values of optical band gap increase from 2.587 to 3.172 eV as the Gd_2O_3 content increases from 1 to 5 mol% (see Fig. 5). The increase in optical band gap is due to the structural changes in the glass network with the addition of trivalent Gd_2O_3. This result suggests that Gd_2O_3 act as a network modifier in the glass system. The polarizing action of the modifying cation, Gd^{3+} ions affects the electronic shell of the O^{2-}. Thus, increasing in the Gd_2O_3 concentration results in progressive increase in the number of bridging oxygens atoms which causes structural changes in the glass network. The increase in the number of bridging oxygen causes the λ_c to shift towards lower wavelength which results in increase of optical band gap. Moreover, the increase in optical band gap energy, E_g, of the present glass could be explained in terms of variation of average bond energy. The increase in the average bond energy of the glass increases the optical band gap of the glasses [17].

Urbach energy, E_U was used to study the degree of disorder in the materials. The materials with higher value of E_U have the tendency to convert weak bond into defects. Due to the potential fluctuations in the disordered material, the band tail allied with the valence band and conduction band is developed which extends into the energy gap and normally shows an exponential behavior. These band tails are characterized by a band tailing parameter and Urbach energy, E_U, given by [18].

$$\alpha(\omega) = B\ \exp(\hbar\omega/E_U) \tag{2}$$

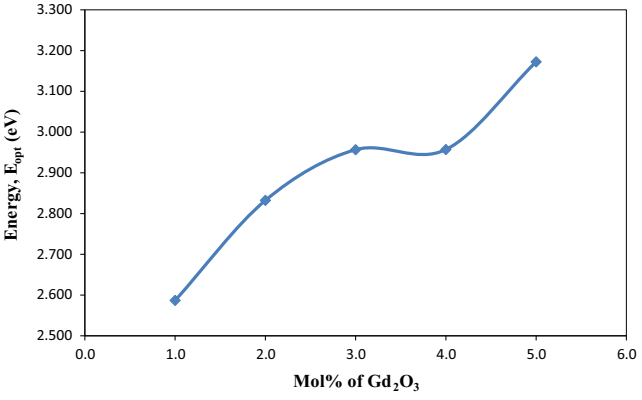

Fig. 5. Indirect optical band gap for TeO_2–B_2O_3–ZnO–Gd_2O_3 glasses.

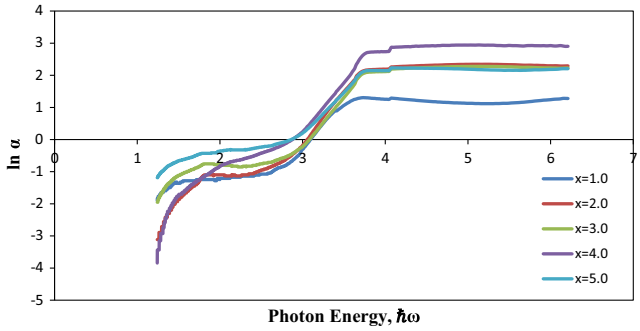

Fig. 6. Variation of ln α with photon energy ħω for TeO_2–B_2O_3–ZnO–Gd_2O_3 glasses.

where B is a constant and E_U is known as band tailing parameter. The values of E_U can be determined as the inverse of the slope of ln α vs ħω plot (Fig. 6) and are listed in Table 3. The values of E_U vary from 0.32 to 0.34 eV. This comparatively small range of E_U is due to phonon-assisted indirect transitions. It is known that the broadening of extinction levels at the absorption level is dominated by the random internal electric field due to lack of long range order and presence of defects in the glass network [18].

The refractive index, n_0 of the glasses can be determined from the following relations [19] and are listed in Table 3:

$$\frac{n_0^2 - 1}{n_0^2 + 2} = 1 - \sqrt{\frac{E_{opt}}{20}} \tag{3}$$

It is seen from Fig. 7 that the refractive indices of the glasses decrease with increasing Gd_2O_3 content. This may be due to effect of large ion concentration of Gd^{3+} ions and formation of dense packing of rare earth modifiers into the host materials. Besides, it can also be attributed to the formation of bridging oxygen which is less polarizable as compared to non-bridging oxygen. The values of refractive index are desirable for fiber optic design and waveguide application. There is an empirical relationship between linear and nonlinear optical susceptibility in solid as proposed by Chen et al. [16]. The large refractive index, n_0, possesses large nonlinear refractive index, n_2.

Nonlinear optical properties

Z-scan technique is a simple approach used to obtain third-order nonlinear optical characteristic of materials. The typical Z-scan normalized transmittance curves for open and closed aperture measurements are shown in Figs. 8 and 9. The values of nonlinear refractive index, n_2 and nonlinear absorption coefficient, β of all the samples can be determined from nonlinear curve fitting. The obtained third order nonlinearities of the samples are recorded in Table 4. Fig. 8 presents the normalized results of the closed-aperture Z-scan. It is shown that a pre-focal transmittance valley followed by a post-focal transmittance peak which shows that these samples perform self-focusing properties and positive refractive nonlinearities [20]. Fig. 10 shows the values of nonlinear refractive index, n_2, initially decrease from 0.9425 to 0.6317×10^{-14} cm^2/W as the concentration of Gd_2O_3 increase from 1 to 2 mol% and increase from 0.6317 to 0.8275×10^{-14} cm^2/W as the Gd_2O_3 increase from 2 to 5 mol%. The variation of nonlinear refractive index, n_2, might be due to highly polarizable cation, Gd^{3+} ions which lead to highly polarizability of the glass network. In addition, the changes in nonlinear refractive index might be due to the easily distorted electron density in a strong electromagnetic field. Hence, the higher value of nonlinear refractive index provides a strong evidence of the contribution of two-photon absorption in the glass network [21–22].

Table 3
Cutoff wavelength for TeO_2–B_2O_3–ZnO–Gd_2O_3 glasses.

x (mol%)	Cutoff wavelength, λ_c (nm)	Optical band gap, E_g^{opt} (eV)	Urbach energy, E_U (eV)	Refractive index, n_0
1.0	419.0	2.587	0.322	2.518
2.0	379.1	2.832	0.327	2.444
3.0	378.8	2.957	0.325	2.409
4.0	372.4	2.957	0.341	2.409
5.0	375.4	3.172	0.340	2.352

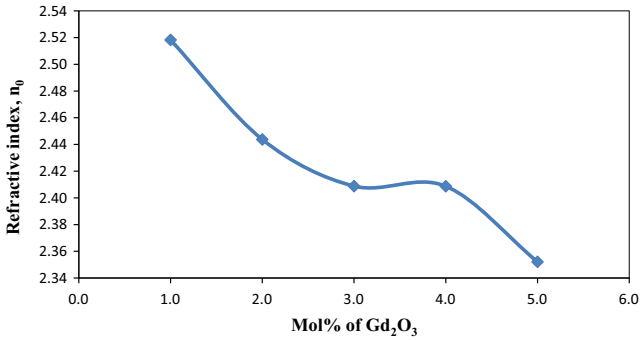

Fig. 7. Refractive index of TeO_2–B_2O_3–ZnO–Gd_2O_3 glasses.

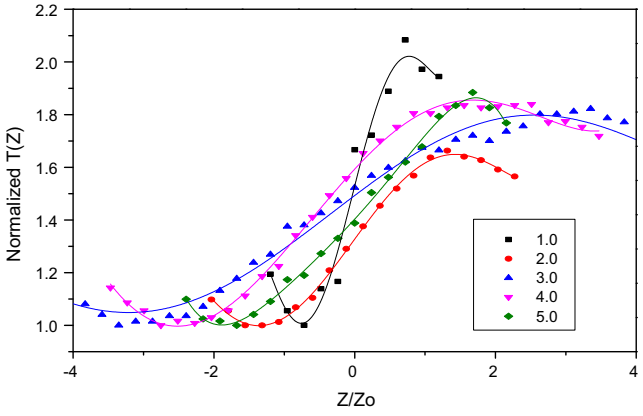

Fig. 8. Closed apertures of TeO_2–B_2O_3–ZnO–Gd_2O_3 glasses.

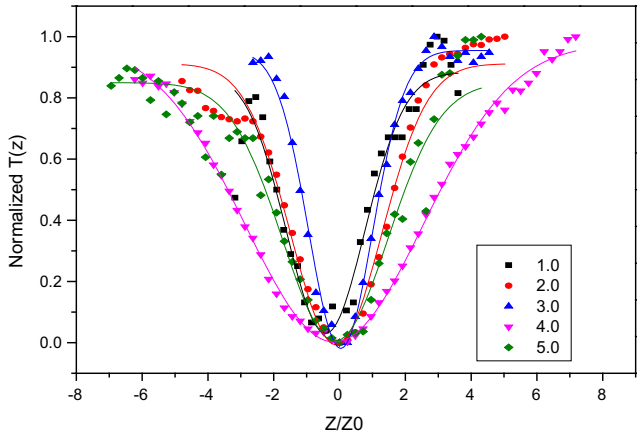

Fig. 9. Open apertures of TeO_2–B_2O_3–ZnO–Gd_2O_3 glasses.

Figs. 9 and 11 represent the normalized results of the open-aperture Z-scan the values of nonlinear absorption coefficient, β, respectively. The values of nonlinear absorption coefficient

Table 4
Nonlinear refractive index, n_2, nonlinear absorption coefficient, β and figure of merit, FOM for TeO_2–B_2O_3–ZnO–Gd_2O_3 glasses.

x (mol% of Gd_2O_3)	n_2 ($\times 10^{-14}$ cm^2/W)	β (cm/GW)	Figure of merit, FOM
1.0	0.9425	0.6157	3.475
2.0	0.6317	0.7117	5.994
3.0	0.7217	0.7466	5.504
4.0	0.8227	0.7142	4.618
5.0	0.8275	0.6460	4.153

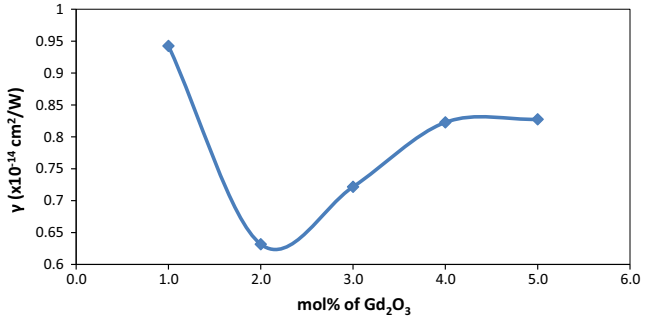

Fig. 10. Nonlinear refractive for TeO_2–B_2O_3–ZnO–Gd_2O_3 glasses.

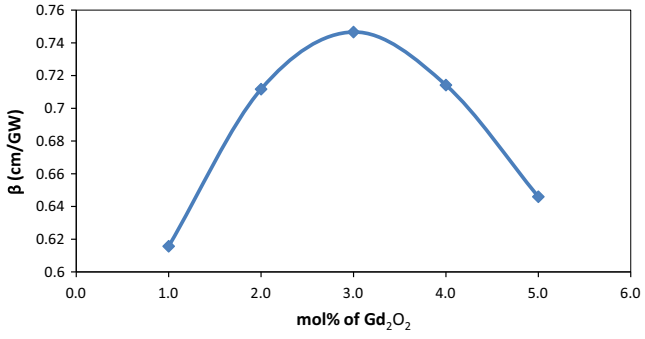

Fig. 11. Nonlinear absorption coefficient for TeO_2–B_2O_3–ZnO–Gd_2O_3 glasses.

increase initially from 0.6157 to 0.7466 $\times$ 10^{-14} cm/GW as the concentration of Gd_2O_3 increase from 1 to 3 mol% and decrease from 0.7466 to 0.6460 $\times$ 10^{-14} cm/GW as the Gd_2O_3 increase from 3 to 5 mol%. The variation of nonlinear absorption coefficient, β is attributed to concurrent formation of TeO_4 and BO_3 structural units in the glass network and the presence lone pair on TeO_4 structure and the effect of large ion Gd^{3+}. The addition of Gd^{3+} ions into the glass network causes conversion of TeO_3 to TeO_4 with the formation of bridging oxygen atoms. The presence of bridging oxygen form strong covalent bond between the molecules in the glass network which results in the increase in nonlinear absorption coefficient. At x = 3.0 mol%, β has the highest value, this might be due to the formation of bridging oxygen which bind the electrons more strongly as compared to the non-bridging oxygen. It might also attribute to the presence of Gd^{3+} ions which are more polarizable

as the concentration of Gd_2O_3 increases. However, further addition of Gd^{3+} ions into the vitreous network causes decrease in density of states above the valence band which leads to decrease in nonlinear absorption coefficient after 3 mol% [17]. Figure of merit (FOM) is used to determine the performance of the nonlinear materials. For two-photon absorption, FOM can be obtained from the expression $\gamma/\beta\lambda$. The values of FOM > 1 can be used to design all-optical switching (AOS) devices while the FOM > 10 is ideal for efficient all-optical devices [22,23]. The values of FOM obtained for the present glasses are recorded in Table 4. It is observed that the presently studied glasses can be used for the design of AOS devices.

Conclusion

Glasses doped with gadolinium oxide were prepared by conventional melt quenching method and their linear and nonlinear properties have been studied. The fundamental absorption edge of these glasses shifted towards lower wavelength due to formation of TeO_4 and BO_4 structural units. The linear optical properties such as optical band gap increases from 2.587 to 3.172 eV whereas the refractive index decreases from 2.518 to 2.352. The changes obtained from optical band gap and refractive index can be related to the structural change of the glass after addition of Gd_2O_3. The third-order optical nonlinearities obtained by Z-scan technique suggested that the presently studied glass can be used for design of all-optical switching devices.

Acknowledgement

The authors wish to acknowledge the financial support from Universiti Putra Malaysia through GPIBT (Geran Putra Individual Berprestasi Tinggi) (9411800).

References

[1] Moawad HMM, Jain H, El-Mallawany R, Ramadan T, El-Sharbiny M. Electrical conductivity of silver vanadium tellurite glasses. J Am Ceram Soc 2002;85:2655–9.
[2] Sidkey MA, El Mallawany RA, Abousehly AA, Saddeek YB. Relaxation of longitudinal ultrasonic waves in some tellurite glasses. Mater Chem Phys 2002;74:222–9.
[3] Abdel-Kader A, El-Mallawany R, Elkholy MM. Network structure of tellurite phosphate glasses: optical absorption and infrared spectra. J Appl Phys 1993;73:71–4.
[4] Bala R, Agarwal A, Sanghi S, Singh N. Effect of Bi_2O_3 on nonlinear optical properties of $ZnO{\cdot}Bi_2O_3{\cdot}SiO_2$ glasses. Opt Mater 2013;36(2):352–6.
[5] El-Deen L, Salhi M, Elkholy M. IR and UV spectral studies for rare earths-doped tellurite glasses. J Alloys Compd 2008;465(1–2):333–9.
[6] Binnemans K, Görller-Walrand C, Adam J. Spectroscopic properties of Gd^{3+}-doped fluorozirconate glass. Chem Phys Lett 1997;280(3–4):333–8.
[7] Jiménez J. Enhanced UV emission of Gd^{3+} in glass by Ag^{+} co-doping. Mater Lett 2015;159:193–6.
[8] Yin M, Li H, Tang S, Ji W. Determination of nonlinear absorption and refraction by single Z-scan method. Appl Phys B 2000;70(4):587–91.
[9] Elkhoshkhany N, Abbas R, El-Mallawany R, Fraih A. Optical Properties of quaternary TeO_2–ZnO–Nb_2O_5–Gd_2O_3 glasses. Ceram Int 2014;40(9):14477–81.
[10] Anand Pandarinath M, Upender G, Narasimha Rao K, Suresh Babu D. Thermal, optical and spectroscopic studies of boro-tellurite glass system containing ZnO. J Non-Cryst Solids 2016;433:60–7.
[11] Suthanthirakumar P, Karthikeyan P, Manimozhi P, Marimuthu K. Structural and spectroscopic behavior of Er^{3+}/Yb^{3+} co-doped boro-tellurite glasses. J Non-Cryst Solids 2015;410:26–34.
[12] Gayathri Pavani P, Sadhana K, Chandra Mouli V. Optical, physical and structural studies of boro-zinc tellurite glasses. Phys B 2011;406(6–7):1242–7.
[13] Abdel-Baki M, El-Diasty F, Wahab F. Optical characterization of $xTiO_2$–$(60-x)SiO_2$–$40Na_2O$ glasses: II. Absorption edge, Fermi level, electronic polarizability and optical basicity. Opt Commun 2006;261(1):65–70.
[14] Rani S, Sanghi S, Ahlawat N, Agarwal A. Influence of Bi_2O_3 on physical, electrical and thermal properties of $Li_2O{\cdot}ZnO{\cdot}Bi_2O_3{\cdot}SiO_2$ glasses. J Alloys Compd 2015;619:659–66.
[15] Ahlawat N, Sanghi S, Agarwal A, Bala R. Influence of SiO_2 on the structure and optical properties of lithium bismuth silicate glasses. J Mol Struct 2010;963(1):82–6.
[16] Chen Y, Nie Q, Xu T, Dai S, Wang X, Shen X. A study of nonlinear optical properties in Bi_2O_3–WO_3–TeO_2 glasses. J Non-Cryst Solids 2008;354(29):3468–72.
[17] Abdel-Baki M, Abdel-Wahab F, El-Diasty F. One-photon band gap engineering of borate glass doped with ZnO for photonics applications. J Appl Phys 2012;111(7):073506.
[18] Ahlawat N, Sanghi S, Agarwal A, Ahlawat N. Influence of SiO_2 on dispersive conductivity and absorption edge of calcium bismuthate glasses. Solid State Ionics 2011;204–205:20–6.
[19] Said Mahraz Z, Sahar M, Ghoshal S. Band gap and polarizability of boro-tellurite glass: influence of erbium ions. J Mol Struct 2014;1072:238–41.
[20] Zhong J, Ma X, Lu H, Wang X, Zhang S, Xiang W. Preparation and optical properties of sodium borosilicate glasses containing Sb nanoparticles. J Alloys Compd 2014;607:177–82.
[21] Guo H, Chen H, Hou C, Lin A, Zhu Y, Lu S, et al. The third-order optical nonlinearities of Ge–Ga–Sb(In)–S chalcogenide glasses. Mater Res Bull 2011;46(5):765–70.
[22] Chen L, Chen F, Dai S, Tao G, Yan L, Shen X, et al. Third-order nonlinearity in Ge–Sb–Se glasses at mid-infrared wavelengths. Mater Res Bull 2015;70:204–8.
[23] Wang T, Gai X, Wei W, Wang R, Yang Z, Shen X, et al. Systematic Z-scan measurements of the third order nonlinearity of chalcogenide glasses. Opt Mater Express 2014;4(5).
[24] Jiménez JA. Enhanced UV emission of Gd^{3+} in glass by Ag^{+} co-doping. Mater Lett 2015;159:193–6.